Langmuir

Article

pubs.acs.org/Langmuir

Vesicle Adhesion and Rupture on Silicon Oxide: Influence of Freeze–Thaw Pretreatment

Joshua A. Jackman,[†,‡] Zhilei Zhao,[†,‡] Vladimir P. Zhdanov,[†,‡,∥] Curtis W. Frank,[⊥] and Nam-Joon Cho*[,†,‡,§]

[†]School of Materials Science and Engineering, Nanyang Technological University, 50 Nanyang Avenue, 639798 Singapore

[‡]Centre for Biomimetic Sensor Science, Nanyang Technological University, 50 Nanyang Drive, 637553 Singapore

[§]School of Chemical and Biomedical Engineering, Nanyang Technological University, 62 Nanyang Drive, 637459 Singapore

[∥]Boreskov Institute of Catalysis, Russian Academy of Sciences, Novosibirsk 630090, Russia

[⊥]Department of Chemical Engineering, Stanford University, Stanford, California 94305, United States

Supporting Information

ABSTRACT: We have investigated the effect of freeze–thaw (FT) pretreatment on the adhesion and rupture of extruded vesicles over a wide range of vesicle sizes. To characterize the size distributions of vesicles obtained with and without FT pretreatment, dynamic light scattering (DLS) experiments were performed. The interaction between extruded vesicles and a silicon oxide substrate was investigated by quartz crystal microbalance with dissipation (QCM-D) monitoring, with a focus on comparative analysis of similar-sized vesicles with and without FT pretreatment. Under this condition, there was a smaller mass load at the critical coverage associated with untreated vesicles, as compared to vesicles which had been subjected to FT pretreatment. In addition, the rupture of treated vesicles generally resulted in formation of a complete planar bilayer, while the adlayer was more heterogeneous when employing untreated vesicles. Combined with kinetic analysis and extended-DLVO model calculations, the experimental evidence suggests that the differences arising from FT pretreatment are due to characteristics of the vesicle size distribution and also multilamellarity of an appreciable fraction of untreated vesicles. Taken together, our findings clarify the influence of FT pretreatment on model membrane fabrication on solid supports.

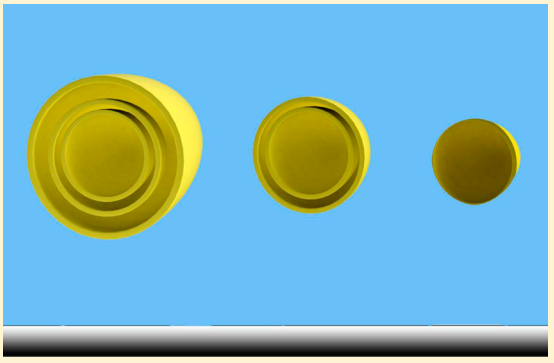

INTRODUCTION

Phospholipid bilayers on solid supports provide a model system to mimic biological membranes and can be studied with surface-sensitive measurement techniques.[1] Fabrication can occur via deposition methods such as the Langmuir–Blodgett transfer process[2] or more commonly vesicle fusion.[3] On hydrophilic supports, the fate of an adsorbed vesicle depends on several factors, including the balance between vesicle–substrate interactions and vesicle bending energy,[4] as well as the line tension associated with the rupture of an adsorbed vesicle.[5−7] Based on the combination of these thermodynamic factors, theory predicts that vesicles above a certain critical size will rupture immediately upon adsorption, whereas smaller vesicles will either adsorb and remain intact or simply not adsorb.[8−10]

While experimental findings support these arguments in some cases,[7,11] theory is still far from complete, and there are deviations between experimental findings and theoretical predictions. Substrate-specific adsorption kinetics of vesicles are experimentally observed largely independent of vesicle size, with various possible channels of vesicle rupture and a dependence on vesicle–substrate, vesicle–vesicle, and vesicle rupture product interactions.[6,12−16] On certain substrates such as silicon oxide[3] and mica,[17] vesicle rupture can occur either spontaneously[13] or after reaching a critical surface coverage.[19] On other substrates such as gold,[3] vesicles can adsorb and remain intact because vesicle rupture is kinetically unfavorable. Hence, there are several channels by which vesicles can adsorb and rupture on solid supports, the rupture process can be controlled energetically, and a wide range of parameters can influence the formation of planar bilayers on solid supports.

Kinetically, the rate of rupture of adsorbed vesicles depends on their deformation. The extent of deformation depends in turn on the dimensionless parameter defined as $w \equiv WR^2/\kappa$, where W is the contact energy per unit area, κ is the membrane bending rigidity, and R is the vesicle radius. Besides vesicle properties (e.g., size,[15] lipid composition,[13] vesicle aging[18]) and substrate properties, the contact energy and corresponding deformation depend on experimental conditions such as temperature,[19] solution pH,[20] ionic strength,[21] ion type,[22] and

Received: December 24, 2013
Revised: February 1, 2014
Published: February 10, 2014

   dx.doi.org/10.1021/la404582n | Langmuir 2014, 30, 2152−2160

osmotic pressure.[23] These conditions can modulate the vesicle−substrate interaction (e.g., via double-layer electrostatic forces) and may therefore influence the state of adsorbed vesicles, including the propensity to rupture. In particular, the deformation of a vesicle is nearly negligible; i.e., its shape is spherical at $w \leq 2$, and with increasing w up to 10, a vesicle becomes boule-shaped with the height approximately 2 times smaller, as compared to the diameter (see, e.g., Figure 1a in ref 8). Physically, vesicle rupture is expected to be faster with increasing w. This is the case if one increases W. With increasing R, the maximum vesicle deformation is, however, nearly independent of R (see, e.g., Monte Carlo simulations[24]), and accordingly, the role of R does not seem to be crucial. Recent simulations[25] based on dissipative particle dynamics indicate that small vesicles are in fact more inclined to rupture.

In all of the experiments quoted above, the conditions used in vesicle preparation were chosen aiming to obtain unilamellar vesicles. However, when dried phospholipids are hydrated in aqueous salt solutions, bi- and multilamellar vesicles (collectively referred to as MLVs) self-assemble spontaneously with a broad size distribution.[26] Several techniques have been developed to control the vesicle size distribution, including sonication[27] and extrusion.[28] Sonication induces an ultrasonic energy wave to form predominately small unilamellar vesicles (SUVs) but has drawbacks, including metal contamination, lipid degradation, and generally produces small vesicles only.[27,29,30] Mechanical extrusion is an alternative technique that can control vesicle size over a wider range. It operates by forcing the passage of MLVs through pores of defined size.[28] MLVs can rupture at the pore entrance[31] and reassemble into smaller, generally unilamellar vesicles with an average size that is reflective of the filter pore size, particularly for small pore sizes.[32] If the pore size is 100 nm or smaller, extrusion will typically produce unilamellar vesicles.[33] By contrast, extrusion through larger pores will generate a more heterogeneous mixture of uni-, bi-, and multilamellar vesicles, as defined by the number of concentric bilayers in a vesicle.[34,35]

To promote unilamellar character among large vesicles, Mayer et al.[36] have subjected vesicles to freeze−thaw (FT) pretreatment before extrusion. During FT pretreatment, vesicles are frozen quickly before being thawed in warm water at a temperature above the gel−liquid crystalline phase transition of the phospholipids. In aqueous salt solutions, this procedure induces bilayer fragmentation of vesicles through an osmotic effect.[37] After five or more cycles, all of the lamellae will have separated in principle, and the MLVs can become predominately unilamellar, even before extrusion.[38] As such, the combination of extrusion and FT pretreatment is able to control both the size and lamellarity of vesicles. Although there are many characterization studies on different types of vesicles in solution, there are no studies focused on the identification of differences in the adsorption and rupture of vesicles obtained with and without FT pretreatment. Furthermore, experimental data concerning how lamellarity affects the adhesion of vesicles onto solid supports are now scarce.[39−41] The corresponding findings generally provide only anecdotal clues that point to the importance of lamellarity to control the adhesion and rupture processes without describing the effects on mechanism.

Herein, using a combination of FT pretreatment and extrusion, we prepared vesicles across a wide size range. Within equivalent size regimes, the adsorption kinetics of vesicles with and without FT pretreatment onto hydrophilic silicon oxide were comparatively studied. Dynamic light scattering (DLS) experiments measured the size distribution of vesicle populations. Quartz crystal microbalance with dissipation (QCM-D) monitoring experiments were performed to monitor the adsorption kinetics of vesicles onto silicon oxide. Taken together with theoretical analysis, the goal of the work was to investigate how the interplay of vesicle lamellarity and size distribution influences the kinetics under consideration.

MATERIALS AND METHODS

Lipid Vesicle Preparation. Vesicles composed of egg phosphatidylcholine (PC) (Avanti Polar Lipids, Alabaster, AL) were prepared at a nominal lipid concentration of ∼5 mg mL^{-1} and then diluted before experiment. Depending on the experiment, vesicles were prepared with either predominately unilamellar or a mixture of unilamellar and multilamellar character by using a previously described methodology based on FT pretreatment and then extrusion.[36] Dried lipid films were hydrated with 10 mM Tris [pH 7.5] buffer solution with 150 mM NaCl, and the sample was then vortexed periodically for 5 min. To produce predominately unilamellar vesicles, FT pretreatment was performed on the newly hydrated lipid films. Specifically, in each treatment cycle, the vesicle suspension was quickly frozen in liquid nitrogen for 30 s, before thawing the suspension in an 80 °C water bath for 90 s, and then finally vortexing to complete each cycle. Typically, seven cycles of FT pretreatment were performed unless otherwise noted. In order to control the size distribution, vesicles were then extruded by repeatedly passing the suspension through a membrane filter with well-defined pore sizes. Vesicles were sized by a miniextruder (Avanti Polar Lipids) through either 1000, 400, 200, 100, or 30 nm polycarbonate membrane pores, depending on the sample. To produce vesicle suspensions with a mixture of uni- and multilamellar character in equivalent size regimes, an identical procedure was performed except there was no FT pretreatment. In this case, after hydration in aqueous salt solution, vesicles were extruded immediately thorough the preferred pore size. All aqueous solutions and buffers were prepared in Milli-Q water with a minimum resistivity of 18.2 MΩ·cm (Millipore, Billerica, MA).

Dynamic Light Scattering. The technique was employed in order to determine the vesicle size distribution based on measuring temporal correlations in the intensity of light scattering by extruded vesicles.[42] The observed intensity is a superposition of the intensities related to individual vesicles. The latter intensity is proportional to the square of the vesicle mass and to the factor depending on the ratio of the vesicle size and wavelength. Temporal changes in the intensity of light scattering by a vesicle are related to diffusion and can be expressed via the diffusion coefficient which, according to hydrodynamics, is inversely proportional to the vesicle radius. In our experiments, a 90Plus particle size analyzer (Brookhaven Instruments, Holtsville, NY) with a 658.0 nm monochromatic laser was employed. In order to minimize the reflection effect, all measurements were taken at the scattering angle of 90°, and the intensity autocorrelation function was measured, which can be fit directly in order to yield the intensity-weighted size distribution of vesicles in solution, as previously described.[42] The autocorrelation function was deconvoluted by using the method of cumulants or the non-negative least squares (NNLS) method. The former method was used to calculate the intensity-weighted Gaussian profile of the vesicle size distribution (including average effective diameter and polydispersity). The latter method was used to calculate the intensity-weighted histogram of the vesicle size distribution. To convert such diagrams into the number-weighted vesicle size distribution, the dependence of the vesicle mass on its size must be known. This dependence is well-known for unilamellar vesicles but often unknown in situations when vesicles are partly or predominantly multilamellar, and their lamellarity is not exactly characterized. For this reason, we present only original intensity-weighted histograms. Concerning this aspect, we note that the contribution of vesicles to such histograms rapidly increases with increasing vesicle size, and accordingly the relative fraction of large vesicles is much smaller than their contribution to an intensity-weighted histogram.

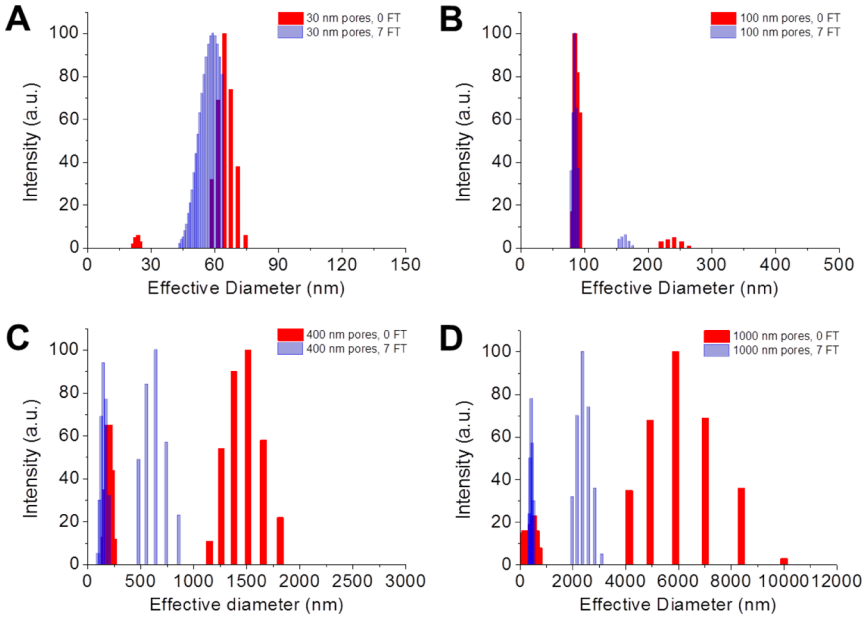

Figure 1. Effects of freeze–thaw pretreatment on DLS intensity-weighted vesicle size distribution. 0 FT (red) and 7 FT (blue) indicate no FT pretreatment or seven cycles of FT pretreatment, respectively. Vesicles were extruded through (A) 30, (B) 100, (C) 400, or (D) 1000 nm pores.

Quartz Crystal Microbalance with Dissipation Monitoring. The adsorption kinetics of vesicles onto silicon oxide were characterized by using the quartz crystal microbalance with dissipation (QCM-D) measurement technique with the Q-Sense D300 instrument (Q-Sense AB, Gothenburg, Sweden) which allows for simultaneous measurement of changes in resonance frequency and energy dissipation as functions of time, as previously described.[43] AT-cut crystals (Q-Sense) of 14 mm diameter with 50 nm thermally evaporated silicon oxide coats were used for all QCM-D experiments. QCM-D crystals were treated with oxygen plasma by using a Plasma Prep 5 plasma cleaner (GaLa Instrumente GmbH, Bad Schwalbach, Germany) at ∼70 W for ∼4 min prior to measurement. Flow cell temperature was maintained at 25.0 °C and controlled by a Peltier element with fluctuations smaller than ±0.02 °C.

RESULTS

Effects of Freeze–Thaw Pretreatment on Vesicle Extrusion Process. Vesicles were prepared with or without FT treatment in order to generate either predominately unilamellar or mixed uni- and multilamellar vesicles, respectively. In order to distinguish between the two cases, where applicable, we refer below to different vesicle suspensions as treated (prepared with FT pretreatment) or untreated (prepared without FT pretreatment). Vesicles were then extruded through different pore sizes (between 30 and 1000 nm diameter) in order to control the vesicle size distribution. Dynamic light scattering experiments were performed in order to determine the effects of FT pretreatment on the size distribution of extruded vesicles (Figure 1).

Small vesicles extruded through 30 nm diameter pores showed minimal effects of FT pretreatment (Figure 1A). The intensity-weighted average diameter was 58 or 60 nm for treated and untreated vesicles, respectively, and there was low polydispersity in both cases. The vesicle sizes are in agreement with past DLS results.[32,34] Moreover, the measurements are consistent with past NMR and freeze-fracture electron microscopy experiments which indicate that extruded vesicles in this size regime are predominately unilamellar.[34] Indeed, due to lipid packing constraints in small vesicles, vesicles in this size regime are intrinsically unilamellar[28] and hence extrusion, in this case, reduces lamellarity independent of FT pretreatment.

When vesicles were extruded through 100 nm pores, FT pretreatment had a more appreciable effect, as noted by intensity-weighted average diameters of 123 and 187 nm for vesicles with and without FT pretreatment, respectively (Figure 1B). In both cases, histogram analysis indicated that there was one subpopulation of vesicles around 85–90 nm diameter and another subpopulation of vesicles with appreciably larger size. For untreated and treated vesicles, the size of the second subpopulation was either around 240 or 165 nm diameter, respectively. The decrease in size of this second subpopulation as the result of FT pretreatment suggests that the vesicles in this larger subpopulation probably have multilamellar character, and FT pretreatment reduces the number of lamellae, as reflected by the size decrease.[35] NMR and freeze-fracture electron microscopy experiments[33,34] have indicated that vesicles extruded through 100 nm pores are predominately unilamellar vesicles. Previous results[46] also support that there is a second, albeit small, subpopulation of larger-size vesicles, as well as the corresponding effect of FT pretreatment. Hence, FT pretreatment improves the generation of vesicles with unilamellar character in this size regime.

Compared to small vesicles (those extruded through 200 nm pores or smaller), FT pretreatment had a more significant effect on the size distribution of large vesicles. When vesicles were extruded through 400 nm pores, the intensity-weighted average diameter was 249 and 478 nm vesicles with and without FT pretreatment, respectively (Figure 1C). The average size for treated vesicles is in agreement with similarly prepared vesicles that were reported in previous work.[34] For both treated and untreated vesicles, there was a bimodal distribution in the intensity-weighted mode. Based on histogram analysis, FT pretreatment affected both subpopulations. Among untreated vesicles, there was one subpopulation around 190 nm diameter and another larger subpopulation around 1511 nm diameter. By contrast, for treated vesicles, the smaller subpopulation had decreased to 151 nm, and the larger subpopulation also

dx.doi.org/10.1021/la404582n | Langmuir 2014, 30, 2152–2160

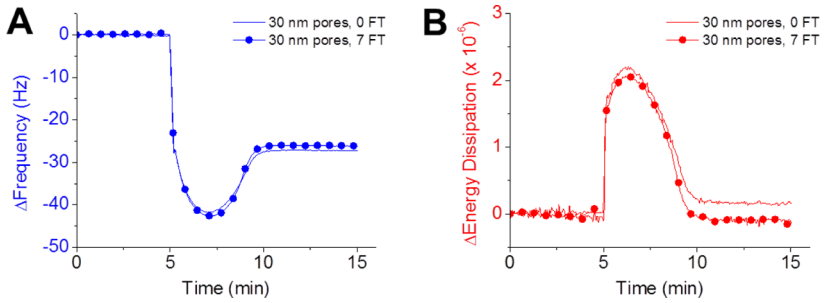

Figure 2. Adhesion of small unilamellar vesicles onto silicon oxide. QCM-D monitoring tracked the change in (A) resonance frequency and (B) energy dissipation as a function of time for treated and untreated vesicles extruded through 30 nm pores.

decreased to 660 nm. The observed changes in vesicle size distribution suggest that the initial mixture of uni- and multilamellar vesicles have increasingly unilamellar character as the result of FT pretreatment.

There are also previous reports[34,35] that seek to determine whether vesicles extruded through 400 nm pores are predominately unilamellar or multilamellar. NMR experiments have estimated that at least 20% of vesicles in this size range are unilamellar if it is conservatively assumed that the multilamellar vesicles are exclusively bilamellar.[34] Jousma et al.[35] have analyzed vesicles extruded through 400 nm pores and determined that there is a large fraction of unilamellar vesicles and a small fraction of multilamellar vesicles with a significant number of lamellae. In addition, it is instructive to consider the physical effects of FT pretreatment. FT pretreatment causes a major structural rearrangement of the vesicle structure with a significant increase in interlamellar spacing and no longer tight packing between bilayers.[36] Indeed, a structural rearrangement has been observed for vesicles extruded through 400 nm pores.[30] Therefore, it must be considered that FT pretreatment affects the vesicle's physical structure as well as the vesicle size distribution.

We also examined the effects of FT pretreatment on appreciably larger vesicles that were extruded through 1000 nm pores (Figure 1D). With FT pretreatment, the intensity-weighted average effective diameter of vesicles decreased from 2005 to 890 nm, which is in agreement with past results.[28] Without FT pretreatment, three subpopulations were identified in the intensity-weighted histogram analysis, corresponding to peak diameters of 171, 495, and 5883 nm. With FT pretreatment, two subpopulations were identified, corresponding to peak diameters of 432 and 2375 nm, respectively. In addition to the change in vesicle size distribution, FT pretreatment also presumably induces a structural arrangement of the lamellae in the vesicles such that the lamellae are no longer tightly packed.

We also performed more detailed studies on how the number of FT cycles affects the properties of extruded vesicles. Vesicles were extruded through 400 nm pores following 0, 1, 3, 5, or 7 cycles of FT pretreatment (Figure S1). The range of intensity-weighted, average diameters ranged from 478 nm without FT pretreatment to 249 nm after seven cycles of FT pretreatment. In all cases, there was a bimodal distribution observed, and both subpopulations decreased in peak size as a function of the cycle number. This trend is consistent with the effects of FT pretreatment, namely that the degree of lamellarity is reduced over a number of cycles.[36] Taken together, the findings support that FT pretreatment generates vesicles with predominately unilamellar character, as defined by the structural rearrangement which increases interlamellar spacing.

In line with the DLS measurement results described above, we consider that unimodal size distributions consist principally of unilamellar vesicles and that multimodal distributions contain appreciable amounts of both uni- and multilamellar vesicles. These findings are in agreement with previous reports on the bimodal size distribution of mildly sonicated vesicles[27,44] and further substantiated by the broad heterogeneity in vesicle size observed in early reports on extruded vesicles.[28]

Adsorption Kinetics of Extruded Vesicles onto Silicon Oxide. We next investigated the effects of FT pretreatment on the adsorption kinetics of vesicles onto silicon oxide. Under the experimental conditions, vesicle adsorption onto silicon oxide typically results in the formation of a planar bilayer which occurs when adsorbed vesicles reach a critical surface coverage and then begin to rupture.[3,45,46] To track the vesicle adsorption process, we employed the QCM-D monitoring technique which measures the change in bound acoustic mass.[3,5,43] The QCM-D experiments were performed over a wide range of vesicle sizes, using the same vesicle populations as mentioned in the previous section. The experimental results are presented in Figures 2−5 and further described below.

For vesicles extruded through 30 nm pores, there was only a minor effect of FT pretreatment on the adsorption kinetics. With or without FT pretreatment, a critical coverage of adsorbed vesicles on the substrate was reached within 3 min when rupture commenced and the formation of a planar bilayer was observed (Figure 2).

This similarity was expected because the DLS experiments showed that the vesicle populations have nearly identical size distributions irrespective of FT treatment. However, there were also differences in the physical properties of the bilayer that are noteworthy. For untreated vesicles, the final changes in resonance frequency and energy dissipation were −28 Hz and 0.2×10^{-6}, respectively. By contrast, for treated vesicles, the final changes in resonance frequency and energy dissipation were −26 Hz and 0.0×10^{-6}, respectively. Hence, FT pretreatment appears to promote the formation of a complete bilayer, and the untreated vesicle population may have a small fraction of vesicles with multilamellar character that do not rupture completely on the substrate. The presence of a small fraction of multilamellar vesicles in this size regime has been previously suggested,[34] and the QCM-D measurements are in line with this conjecture. Therefore, FT pretreatment improves bilayer quality even in the small-size vesicle regime.

Vesicles extruded through 100 nm pores also showed similar adsorption kinetics with or without FT pretreatment, albeit with more significant differences than vesicles in the smallest

dx.doi.org/10.1021/la404582n | Langmuir 2014, 30, 2152−2160

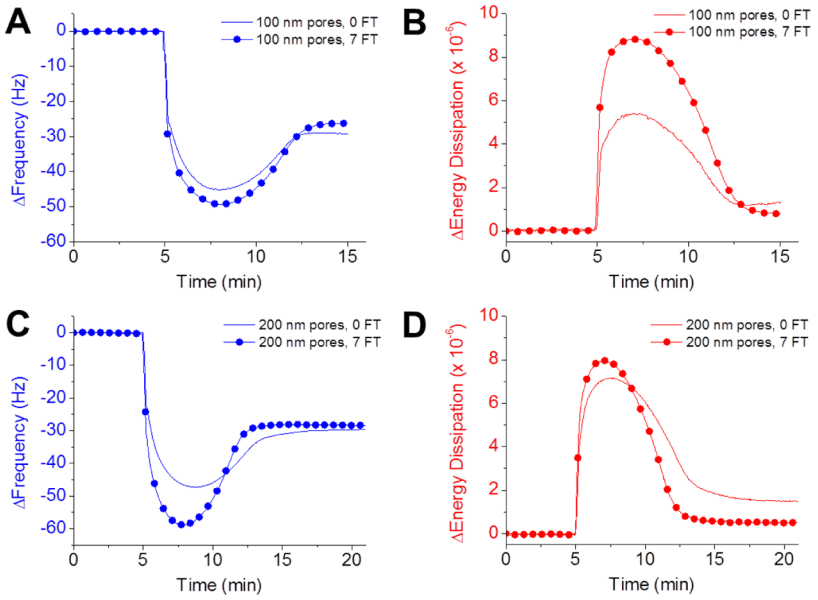

Figure 3. Freeze–thaw pretreatment affects adhesion of intermediate size vesicles. QCM-D monitoring tracked the change in (A) resonance frequency and (B) energy dissipation as a function of time for treated and untreated vesicles extruded through 100 nm pores. Panels (C) and (D) show similar results for vesicles extruded through 200 nm pores.

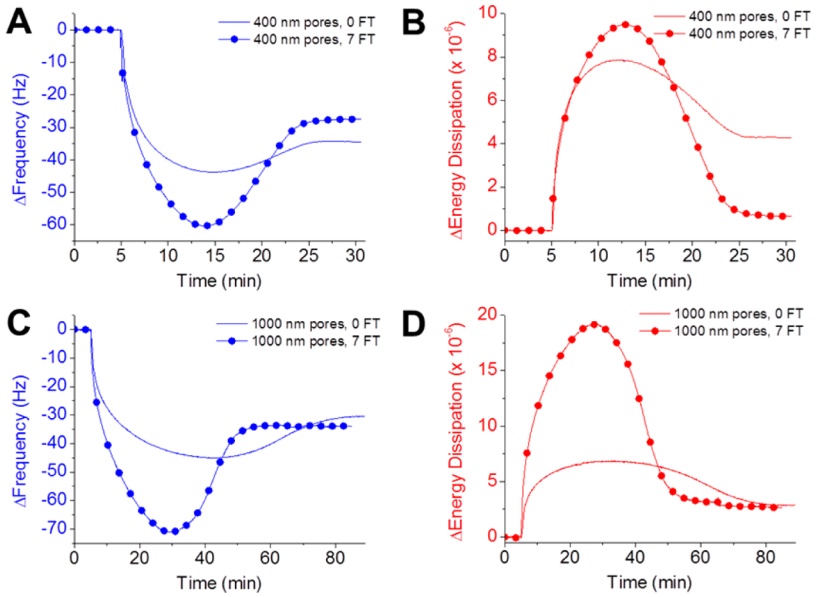

Figure 4. Effects of lamellarity and size distribution on the adhesion of large vesicles onto silicon oxide. QCM-D monitoring tracked the change in (A) resonance frequency and (B) energy dissipation as a function of time for vesicles extruded through 400 nm pores. Panels (C) and (D) exhibit similar results for vesicles extruded through 1000 nm pores.

size regime tested (Figure 3A,B). Although adsorption behavior related to the critical coverage was similar, there were deviations in the final changes in resonance frequency and energy dissipation. The rupture of untreated vesicles resulted in final changes in resonance frequency and energy dissipation of −32 Hz and 1×10^{-6}, respectively. By contrast, the rupture of treated vesicles resulted in final changes in resonance frequency and energy dissipation of −28 Hz and 0.5×10^{-6}, respectively. The former corresponds to a planar bilayer with a significant number of unruptured vesicles present while the latter is more representative of a completely formed bilayer, albeit still with some unruptured vesicles likely present. Therefore, adhesion and rupture by treated vesicles is preferred to form bilayers.

A similar trend in bilayer formation was also observed for vesicles extruded through 200 nm pores, although differences between the vesicle populations with and without FT treatment were more significant and FT pretreatment also influenced the critical coverage more appreciably (Figure 3C,D). Untreated vesicles reached a critical coverage that corresponded to changes in resonance frequency and energy dissipation of −45 Hz and 7×10^{-6}, respectively, versus changes in resonance frequency and energy dissipation of −58 Hz and 9×10^{-6}, respectively, for treated vesicles. Again, as with vesicles extruded through 100 nm pores, treated vesicles formed a more complete bilayer than untreated vesicles. The final changes in resonance frequency and energy dissipation were −30 Hz and 2

dx.doi.org/10.1021/la404582n | *Langmuir* 2014, 30, 2152–2160

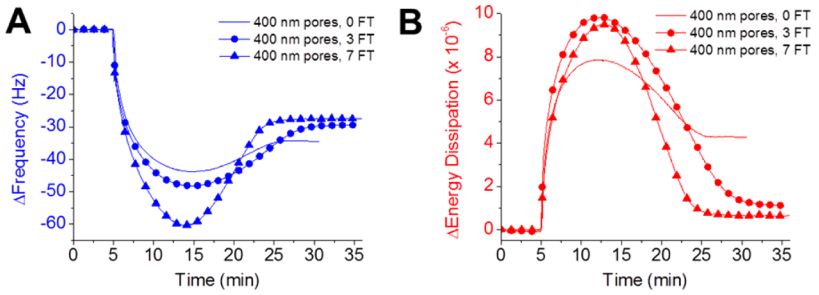

Figure 5. Relative degree of lamellarity influences vesicle adsorption kinetics. QCM-D monitoring tracked the change in (A) resonance frequency and (B) energy dissipation as a function of time for vesicles extruded through 400 nm pores after 0, 3, or 7 FT pretreatment cycles.

$\times 10^{-6}$, respectively, for untreated vesicles, and −28 Hz and 1×10^{-6}, respectively, for treated vesicles. As such, FT pretreatment clearly improves the quality of formed bilayers on the basis of the QCM-D measurement values.

We also tested the adsorption kinetics of larger vesicles extruded through 400 or 1000 nm pores (Figure 4). These larger size vesicles also showed the same trends in adsorption kinetics as smaller vesicles, albeit with more pronounced effects of FT pretreatment. For vesicles extruded through 400 nm pores, treated vesicles reached a critical coverage that corresponded to changes in resonance frequency and energy dissipation of −60 Hz and 10×10^{-6}, respectively, versus changes in resonance frequency and energy dissipation of −43 Hz and 8×10^{-6}, respectively, for untreated vesicles (Figure 4A,B). The final changes in resonance frequency and energy dissipation were −36 Hz and 4.5×10^{-6}, respectively, for untreated vesicles and −28 Hz and 0.7×10^{-6}, respectively, for treated vesicles. Hence, for larger vesicle sizes, the effects of FT pretreatment on vesicle rupture were more significant.

To further examine the effects of vesicle size dependence, we also investigated vesicles extruded through 1000 nm pores (Figure 4C,D). Treated vesicles reached a critical coverage that corresponded to changes in resonance frequency and energy dissipation of −72 Hz and 19×10^{-6}, respectively, versus changes in resonance frequency and energy dissipation of −44 Hz and 6×10^{-6}, respectively, for untreated vesicles. The final changes in resonance frequency and energy dissipation were −36 Hz and 3×10^{-6}, respectively, for untreated vesicles and −28 Hz and 3×10^{-6}, respectively, for treated vesicles. In this limiting size regime, it appears that additional factors such as vesicle sterics also play a significant role to influence the degree of bilayer formation.

In addition to measuring the effects of FT pretreatment on the adsorption kinetics of vesicles, we also examined the effect of the number of FT pretreatment cycles (Figure 5). Using vesicles extruded through 400 nm pores, we tested how the number of FT pretreatment cycles affects the adsorption kinetics of vesicles onto silicon oxide. Without FT pretreatment, the interaction of lipid vesicles with silicon oxide results in vesicle rupture and the formation of an incomplete bilayer with final changes in resonance frequency and energy dissipation of −37 Hz and 4.3×10^{-6}, respectively. For vesicles subjected to three FT pretreatment cycles, vesicle rupture led to final changes in resonance frequency and energy dissipation of −31 Hz and 1.2×10^{-6}, respectively. As the physical properties of the vesicle adlayer at the critical coverage were similar, the differences in the final mass values following adhesion and rupture are likely due to variations in the rupture mechanism. In contrast to these two cases, vesicles subjected to seven FT pretreatment cycles had a significantly greater mass load at the critical coverage, and vesicle rupture resulted in the formation of a relatively complete bilayer with final changes in resonance frequency and energy dissipation of −28 Hz and 0.9×10^{-6}, respectively.

DISCUSSION

Our experiments have specified how FT pretreatment influences vesicle properties and their interactions with solid supports. For vesicles with single populations, the effect of FT pretreatment was limited, presumably because these vesicles are typically small and predominately unilamellar. However, for vesicles with multiple subpopulations, FT pretreatment influenced vesicle size characteristics, including the average vesicle size in each subpopulation along with the relative variance between the two subpopulations. Accordingly, FT pretreatment affected the adsorption kinetics of vesicles onto silicon oxide. Untreated vesicles had generally smaller mass loads at the critical coverage and did not form complete planar bilayers. By contrast, treated vesicles had greater mass loads at the critical coverage but ruptured to form more complete planar bilayers. We discuss these findings in relation to two factors, adsorption kinetics and rupture mechanism, and focus attention on the role of vesicle lamellarity.

There was a difference in the adsorption kinetics of untreated and treated vesicles, which was particularly evident at the critical coverage. To analyze the vesicle−substrate interaction at the critical coverage, we focused on the contact area between vesicles and the substrate. Within this scope, the vesicle can be represented as a planar bilayer on the substrate and the total interaction energy between the bilayer and substrate may be estimated.[47] Extended-DLVO models have been applied to reasonably approximate this case based on three interfacial forces, namely the van der Waals, double-layer electrostatic, and hydration forces.[48−50] As described in the Supporting Information, we employed herein a modified approach[50,51] that accounts for multiple bilayers on a substrate as would be expected for a multilamellar vesicle.

In our context, we may note that the vesicles and substrate used are negatively charged.[47] Although the surface charge concentration is relatively low in both cases, the contribution of the double-layer electrostatic force to the interaction of the external leaflet of a vesicle with the substrate is not fully negligible. Comparing e.g. uni- and bilamellar vesicles, we may add that the electrostatic interaction of the additional internal bilayer of a bilamellar vesicle with the substrate is repulsive, albeit marginally small. Accordingly, this interaction cannot explain why the mass load at the critical coverage is lower with increasing multilamellarity (i.e., for vesicles with fewer FT

dx.doi.org/10.1021/la404582n | Langmuir 2014, 30, 2152−2160

pretreatment cycles). By contrast, the van der Waals interaction of the additional internal bilayer of a bilamellar vesicle with the substrate is attractive. This interaction, however, rapidly decreases with increasing distance between the bilayer and substrate. For this reason, the total van der Waals energy (per unit area) will increase only slightly. All of these arguments have been confirmed by our extended-DLVO model calculations of the total interaction energy between individual bilayers within a multilamellar vesicle (up to $n = 4$ bilayers where $n = 1$ is the bilayer closest to the substrate) and the corresponding silicon oxide substrate (Figure 6).

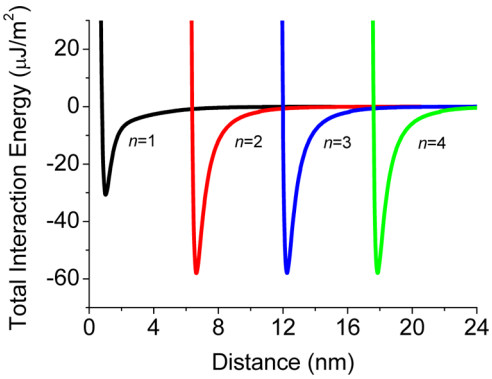

Figure 6. Extended-DLVO model of a multilamellar vesicle on silicon oxide. Total interaction energy of the nth lipid bilayer with the substrate and underlying bilayers is plotted as a function of the bilayer−substrate separation distance for $n \leq 4$.

Based on the model calculations, the interaction between the outermost bilayer and the substrate has a total interaction energy of -31 μJ/m^2. By contrast, the total interaction energy of inner bilayers is always -58 μJ/m^2, which is appreciably larger than the oxide−bilayer interaction of the outermost bilayer. The consistency of this value for all inner bilayers supports that the interaction between inner bilayers and the substrate is largely negligible as is the interaction between bilayers beyond the nearest-neighboring bilayer (Table 1). The

Table 1. Summary of Values of Extended-DLVO Model Calculations for Multilamellar Vesicles on Silicon Oxide[a]

extended-DLVO model parameter	bilayer ($n = 1$)	bilayer ($n = 2$)	bilayer ($n = 3$)	bilayer ($n = 4$)
equilib distance (nm)	1.03	6.64	12.25	17.86
equilib energy (μJ/m^2)	−30.69	−58.01	−57.94	−57.93
contribution to oxide−bilayer interaction energy (μJ/m^2)	−30.69	−0.88	−0.17	−0.06

[a]Values are based on graph presented in Figure 6.

key contribution to the total interaction energy of inner bilayers is the bilayer−bilayer interaction. Therefore, it appears that the presence of additional bilayers inside a multilamellar vesicle does not increase the vesicle−substrate interaction.

It must also be considered that the bending rigidity of a bilamellar vesicle is about 2 times larger than that of a unilamellar vesicle[52] (provided that the sizes of the bilayers in a bilamellar vesicle are comparable, which we assume is the case without FT pretreatment). As previously noted in the Introduction, the extent of vesicle deformation increases with increasing $w \equiv WR^2/\kappa$. Accordingly, for bilamellar or multilamellar vesicles, the increase in W is fully compensated by the increase in κ. Thus, bilamellar or multilamellar vesicles are expected to be less deformed, and accordingly, the increase in total interaction energy also cannot explain why the mass load at the critical coverage is lower with increasing lamellarity.

To explain why the mass load at the critical coverage is lower in the case of untreated vesicles (i.e., those with greater multilamellarity), we note an additional characteristic of these vesicles is that they generally consist of two subpopulations with an appreciable difference in the average size corresponding to each subpopulation. The concentration of vesicles belonging to the small-size subpopulation is much larger and they diffuse toward the surface much faster. For this reason, the adlayer primarily contains vesicles from the small-size subpopulation. The vesicles belonging to the large-size subpopulation also arrive at the surface although at a much lower rate. With increasing surface concentration of small-size vesicles, the steric constraints for adsorption of large-size vesicles may become appreciable already at a relatively small surface concentration of the former vesicles. The thermodynamic driving force for adsorption of large-size vesicles is, however, high due to their large membrane surface area. Under such circumstances, the steric constraints may initiate rupture of large-size vesicles, and the latter may in turn induce rupture of small-size vesicles, e.g., at the boundaries of lipid islands (this mechanism of rupture is discussed in detail in ref 12 and observed recently in ref 53). In this case, the reason why the mass load at the critical coverage is lower for untreated vesicles is because the vesicles have a bimodal size distribution, and there is a large difference in vesicle size between the two subpopulations. Vesicle lamellarity may nevertheless play an important role because it may influence the state of the adlayer after reaching the critical coverage and vesicles rupture. Indeed, it must be considered that this model is only valid to explain the observed mass loads corresponding to the critical coverage and does not describe in detail subsequent events. Hence, additional factors must be involved to explain the outcome of the vesicle rupture process.

Concerning our observations that untreated vesicles do not form a complete bilayer whereas treated vesicles generally form a complete bilayer, we note that previous studies of related systems have shown that multilamellar vesicles, which are more predominant among untreated vesicles, have a broad rupture profile, as evidenced by a large scattering in rupture kinetics.[39−41] While these studies have suggested that heterogeneity of multilamellar vesicles is a key issue, the rupture process of multilamellar vesicles is also intrinsically more complex than that of unilamellar vesicles because there are multiple lamellae. The rupture of the outermost lamella is a competition between the energetics of the lipid−substrate interaction versus the collective energetics of the interlamella interaction (assuming the bilayers are tightly packed in the multilamellar vesicle). Therefore, a ruptured, multilamellar vesicle may remain largely intact on the substrate and contribute a viscoelastic element to the adlayer properties. An additional effect would be that a high coverage of multilamellar vesicles may act as a steric barrier to prevent the rupture of nearby vesicles.[28] Taken together, there are multiple pathways by which multilamellarity may hinder the formation of a complete bilayer, thereby underscoring the general utility of FT pretreatment to promote unilamellar character and improve planar bilayer formation.

dx.doi.org/10.1021/la404582n | Langmuir 2014, 30, 2152−2160

CONCLUSION

In this work, we have investigated the effects of FT pretreatment on vesicle size properties and adsorption kinetics of extruded vesicles onto silicon oxide. Through comparative analysis of treated and untreated vesicles in equivalent size regimes, we identified several factors which are influenced by FT pretreatment. Treated vesicles generally had smaller size than untreated vesicles. For large-size vesicles with multiple subpopulations, including one or more subpopulations containing multilamellar vesicles, FT pretreatment generally led to a decrease in the average vesicle size in each subpopulation along with a decrease in the relative variance between the subpopulations. As a result, the critical coverage corresponding to untreated vesicles had a lower mass load because there appears to be a greater thermodynamic driving force for the rupture of large-size vesicles in the presence of predominantly small-size vesicles on the surface. However, an increased propensity to rupture did not always lead to formation of a complete bilayer. Treated vesicles were preferred to form complete bilayers in all size regimes, including among small vesicles. Hence, to summarize, promoting unilamellar character by way of FT pretreatment can improve the formation of planar bilayers on silicon oxide in a manner which is independent of vesicle size. All of these details clarify the influence of FT pretreatment on vesicle preparation and its corresponding utility for model membrane fabrication.

ASSOCIATED CONTENT

Supporting Information

More detailed information about DLS experiments (Figure S1) and extended-DLVO model calculations (Figures S2–S4). This material is available free of charge via the Internet at http://pubs.acs.org.

AUTHOR INFORMATION

Corresponding Author

*E-mail: njcho@ntu.edu.sg (N.-J.C.).

Notes

The authors declare no competing financial interest.

ACKNOWLEDGMENTS

The authors acknowledge support from the National Research Foundation (NRF-NRFF2011-01), the National Medical Research Council (NMRC/CBRG/0005/2012), and Nanyang Technological University to N.J.C. J.A.J. is a recipient of the Nanyang President's Graduate Scholarship. V.P.Zh. is a recipient of the Tan Chin Tuan Exchange Fellowship at Nanyang Technological University.

REFERENCES

(1) Sackmann, E. Supported membranes: Scientific and practical applications. *Science* **1996**, *271* (5245), 43–48.
(2) von Tscharner, V.; McConnell, H. M. Physical properties of lipid monolayers on alkylated planar glass surfaces. *Biophys. J.* **1981**, *36* (2), 421–427.
(3) Keller, C.; Kasemo, B. Surface specific kinetics of lipid vesicle adsorption measured with a quartz crystal microbalance. *Biophys. J.* **1998**, *75* (3), 1397–1402.
(4) Zhdanov, V.; Kasemo, B. Comments on rupture of adsorbed vesicles. *Langmuir* **2001**, *17* (12), 3518–3521.
(5) Cho, N.-J.; Frank, C. W.; Kasemo, B.; Höök, F. Quartz crystal microbalance with dissipation monitoring of supported lipid bilayers on various substrates. *Nat. Protoc.* **2010**, *5* (6), 1096–1106.
(6) Richter, R. P.; Bérat, R.; Brisson, A. R. Formation of solid-supported lipid bilayers: an integrated view. *Langmuir* **2006**, *22* (8), 3497–3505.
(7) Muresan, A. S.; Lee, K. Y. C. Shape evolution of lipid bilayer patches adsorbed on mica: an atomic force microscopy study. *J. Phys. Chem. B* **2001**, *105* (4), 852–855.
(8) Seifert, U.; Lipowsky, R. Adhesion of vesicles. *Phys. Rev. A* **1990**, *42* (8), 4768.
(9) Lipowsky, R.; Seifert, U. Adhesion of vesicles and membranes. *Mol. Cryst. Liq. Cryst.* **1991**, *202* (1), 17–25.
(10) Seifert, U. Configurations of fluid membranes and vesicles. *Adv. Phys.* **1997**, *46* (1), 13–137.
(11) Egawa, H.; Furusawa, K. Liposome adhesion on mica surface studied by atomic force microscopy. *Langmuir* **1999**, *15* (5), 1660–1666.
(12) Zhdanov, V. P.; Keller, C.; Glasmästar, K.; Kasemo, B. Simulation of adsorption kinetics of lipid vesicles. *J. Chem. Phys.* **2000**, *112*, 900.
(13) Richter, R.; Mukhopadhyay, A.; Brisson, A. Pathways of lipid vesicle deposition on solid surfaces: a combined QCM-D and AFM study. *Biophys. J.* **2003**, *85* (5), 3035–3047.
(14) Johnson, J. M.; Ha, T.; Chu, S.; Boxer, S. G. Early steps of supported bilayer formation probed by single vesicle fluorescence assays. *Biophys. J.* **2002**, *83* (6), 3371–3379.
(15) Reimhult, E.; Hook, F.; Kasemo, B. Vesicle adsorption on SiO_2 and TiO_2: Dependence on vesicle size. *J. Chem. Phys.* **2002**, *117* (16), 7401–7404.
(16) Reimhult, E.; Zäch, M.; Höök, F.; Kasemo, B. A multitechnique study of liposome adsorption on Au and lipid bilayer formation on SiO_2. *Langmuir* **2006**, *22* (7), 3313–3319.
(17) Reviakine, I.; Brisson, A. Formation of supported phospholipid bilayers from unilamellar vesicles investigated by atomic force microscopy. *Langmuir* **2000**, *16* (4), 1806–1815.
(18) Cho, N.-J.; Hwang, L. Y.; Solandt, J. J.; Frank, C. W. Comparison of extruded and sonicated vesicles for planar bilayer self-assembly. *Materials* **2013**, *6* (8), 3294–3308.
(19) Reimhult, E.; Höök, F.; Kasemo, B. Temperature dependence of formation of a supported phospholipid bilayer from vesicles on SiO_2. *Phys. Rev. E* **2002**, *66* (5), 051905.
(20) Cho, N.-J.; Jackman, J. A.; Liu, M.; Frank, C. W. pH-Driven assembly of various supported lipid platforms: a comparative study on silicon oxide and titanium oxide. *Langmuir* **2011**, *27* (7), 3739–3748.
(21) Boudard, S.; Seantier, B.; Breffa, C.; Decher, G.; Felix, O. Controlling the pathway of formation of supported lipid bilayers of DMPC by varying the sodium chloride concentration. *Thin Solid Films* **2006**, *495* (1), 246–251.
(22) Richter, R. P.; Brisson, A. R. Following the formation of supported lipid bilayers on mica: a study combining AFM, QCM-D, and ellipsometry. *Biophys. J.* **2005**, *88* (5), 3422–3433.
(23) Reimhult, E.; Höök, F.; Kasemo, B. Intact vesicle adsorption and supported biomembrane formation from vesicles in solution: Influence of surface chemistry, vesicle size, temperature, and osmotic pressure. *Langmuir* **2003**, *19* (5), 1681–1691.
(24) Dimitrievski, K. Deformation of adsorbed lipid vesicles as a function of vesicle size. *Langmuir* **2010**, *26* (5), 3008–3011.
(25) Wu, H.-L.; Chen, P.-Y.; Chi, C.-L.; Tsao, H.-K.; Sheng, Y.-J. Vesicle deposition on hydrophilic solid surfaces. *Soft Matter* **2013**, *9* (6), 1908–1919.
(26) Bangham, A. Properties and uses of lipid vesicles: an overview. *Ann. N. Y. Acad. Sci.* **1978**, *308* (1), 2–7.
(27) Huang, C.-H. Phosphatidylcholine vesicles. Formation and physical characteristics. *Biochemistry* **1969**, *8* (1), 344–352.
(28) Olson, F.; Hunt, C.; Szoka, F.; Vail, W.; Papahadjopoulos, D. Preparation of liposomes of defined size distribution by extrusion through polycarbonate membranes. *Biochim. Biophys. Acta, Biomembr.* **1979**, *557* (1), 9–23.
(29) Hope, M.; Bally, M.; Mayer, L.; Janoff, A.; Cullis, P. Generation of multilamellar and unilamellar phospholipid vesicles. *Chem. Phys. Lipids* **1986**, *40* (2), 89–107.

(30) Mui, B.; Chow, L.; Hope, M. J. Extrusion technique to generate liposomes of defined size. *Methods Enzymol.* **2003**, *367*, 3−14.
(31) Frisken, B.; Asman, C.; Patty, P. Studies of vesicle extrusion. *Langmuir* **2000**, *16* (3), 928−933.
(32) MacDonald, R. C.; MacDonald, R. I.; Menco, B. P. M.; Takeshita, K.; Subbarao, N. K.; Hu, L.-r. Small-volume extrusion apparatus for preparation of large, unilamellar vesicles. *Biochim. Biophys. Acta, Biomembr.* **1991**, *1061* (2), 297−303.
(33) Hope, M.; Bally, M.; Webb, G.; Cullis, P. Production of large unilamellar vesicles by a rapid extrusion procedure. Characterization of size distribution, trapped volume and ability to maintain a membrane potential. *Biochim. Biophys. Acta, Biomembr.* **1985**, *812* (1), 55−65.
(34) Mayer, L.; Hope, M.; Cullis, P. Vesicles of variable sizes produced by a rapid extrusion procedure. *Biochim. Biophys. Acta, Biomembr.* **1986**, *858* (1), 161−168.
(35) Jousma, H.; Talsma, H.; Spies, F.; Joosten, J.; Junginger, H.; Crommelin, D. Characterization of liposomes. The influence of extrusion of multilamellar vesicles through polycarbonate membranes on particle size, particle size distribution and number of bilayers. *Int. J. Pharm.* **1987**, *35* (3), 263−274.
(36) Mayer, L.; Hope, M.; Cullis, P.; Janoff, A. Solute distributions and trapping efficiencies observed in freeze-thawed multilamellar vesicles. *Biochim. Biophys. Acta, Biomembr.* **1985**, *817* (1), 193−196.
(37) MacDonald, R. C.; Jones, F. D.; Qui, R. Fragmentation into small vesicles of dioleoylphosphatidylcholine bilayers during freezing and thawing. *Biochim. Biophys. Acta, Biomembr.* **1994**, *1191* (2), 362−370.
(38) Traïkia, M.; Warschawski, D. E.; Recouvreur, M.; Cartaud, J.; Devaux, P. F. Formation of unilamellar vesicles by repetitive freeze-thaw cycles: characterization by electron microscopy and ^{31}P-nuclear magnetic resonance. *Eur. Biophys. J.* **2000**, *29* (3), 184−195.
(39) Agmo Hernández, V.; Scholz, F. Kinetics of the adhesion of DMPC liposomes on a mercury electrode. Effect of lamellarity, phase composition, size and curvature of liposomes, and presence of the pore forming peptide mastoparan X. *Langmuir* **2006**, *22* (25), 10723−10731.
(40) Gulcev, M. D.; Lucy, C. A. Factors affecting the behavior and effectiveness of phospholipid bilayer coatings for capillary electrophoretic separations of basic proteins. *Anal. Chem.* **2008**, *80* (5), 1806−1812.
(41) Hellberg, D.; Scholz, F.; Schubert, F.; Lovric, M.; Omanovic, D.; Hernández, V. A.; Thede, R. Kinetics of liposome adhesion on a mercury electrode. *J. Phys. Chem. B* **2005**, *109* (30), 14715−14726.
(42) Pencer, J.; Hallett, F. R. Effects of vesicle size and shape on static and dynamic light scattering measurements. *Langmuir* **2003**, *19* (18), 7488−7497.
(43) Rodahl, M.; Hook, F.; Krozer, A.; Brzezinski, P.; Kasemo, B. Quartz crystal microbalance setup for frequency and Q-factor measurements in gaseous and liquid environments. *Rev. Sci. Instrum.* **1995**, *66* (7), 3924−3930.
(44) Woodbury, D. J.; Richardson, E. S.; Grigg, A. W.; Welling, R. D.; Knudson, B. H. Reducing liposome size with ultrasound: bimodal size distributions. *J. Liposome Res.* **2006**, *16* (1), 57−80.
(45) Keller, C.; Glasmästar, K.; Zhdanov, V.; Kasemo, B. Formation of supported membranes from vesicles. *Phys. Rev. Lett.* **2000**, *84* (23), 5443−5446.
(46) Morigaki, K.; Tawa, K. Vesicle fusion studied by surface plasmon resonance and surface plasmon fluorescence spectroscopy. *Biophys. J.* **2006**, *91* (4), 1380−1387.
(47) Jackman, J. A.; Choi, J.-H.; Zhdanov, V. P.; Cho, N.-J. Influence of osmotic pressure on adhesion of lipid vesicles to solid supports. *Langmuir* **2013**, *29* (36), 11375−11384.
(48) Nabika, H.; Fukasawa, A.; Murakoshi, K. Tuning the dynamics and molecular distribution of the self-spreading lipid bilayer. *Phys. Chem. Chem. Phys.* **2008**, *10* (16), 2243−2248.
(49) Tero, R.; Ujihara, T.; Urisu, T. Lipid bilayer membrane with atomic step structure: supported bilayer on a step-and-terrace TiO_2 (100) surface. *Langmuir* **2008**, *24* (20), 11567−11576.
(50) Oleson, T. A.; Sahai, N. Interaction energies between oxide surfaces and multiple phosphatidylcholine bilayers from extended-DLVO theory. *J. Colloid Interface Sci.* **2010**, *352* (2), 316−326.
(51) Oleson, T. A.; Sahai, N.; Pedersen, J. A. Electrostatic effects on deposition of multiple phospholipid bilayers at oxide surfaces. *J. Colloid Interface Sci.* **2010**, *352* (2), 327−336.
(52) De Haas, K.; Blom, C.; Van den Ende, D.; Duits, M.; Mellema, J. Deformation of giant lipid bilayer vesicles in shear flow. *Phys. Rev. E* **1997**, *56* (6), 7132−7137.
(53) Andrecka, J.; Spillane, K. M.; Ortega-Arroyo, J.; Kukura, P. Direct Observation and Control of Supported Lipid Bilayer Formation with Interferometric Scattering Microscopy. *ACS Nano* **2013**, *7* (12), 10662−10670.